Efficient Generation of Puncturing-Assisted Rate-Matched 5G New Radio LDPC Codes for Faster-Than-Nyquist Signaling

Asma A. Alqudah[1,*], Khaled F. Hayajneh[1,2], Hasan A. Aldiabat[1], and Hazim M. Shakhatreh[1]

[1]Telecommunications Engineering Department, Yarmouk University, Irbid, Jordan
[2]College of Engineering and Technology, American University of the Middle East, Egaila 54200, Kuwait
Emails: asma.qudah @yu.edu.jo (A.A.A.); khaled.hayajneh@aum.edu.kw (K.F.H.); hasan.aldiabat@yu.edu.jo (H.A.A.); hazim.s@yu.edu.jo (H.M.S.)
*Corresponding author

***Abstract*—This paper presents a comprehensive analysis of the utilization of rate-matched 5G New Radio (NR) Low-Density Parity Check (LDPC) codes for decoding faster-than-Nyquist signaled data symbols in an Additive White Gaussian Noise (AWGN) channel. The rate-matching techniques employing message-bit and parity-bit puncturing are thoroughly explained, showcasing the applications of various rates during the coding process. Moreover, in conjunction with the aforementioned rate-matching and puncturing methods, a puncturing scheme is employed on the first two columns of the parity-check matrix derived from the 5G NR LDPC base graphs. The performance of the 5G NR LDPC code, integrated as the outer decoder in turbo equalization for faster-than-Nyquist signaled data symbols, is thoroughly investigated. The achieved results are compared with the performance of convolutional codes implemented in the same system setup and operating at identical code rates. By analyzing the employment of rate-matched 5G NR LDPC codes, this paper provides valuable insights into their efficacy for decoding faster-than-Nyquist signaled data symbols in the AWGN channel. The comparison with convolutional codes offers a benchmark for performance evaluation, facilitating a deeper understanding of the benefits and trade-offs associated with each coding scheme.**

***Keywords*—Faster-than-Nyquist, 5G New Radio (NR) Low-Density Parity Check (LDPC) codes, rate-matching, puncturing, turbo equalization**

I. Introduction

Faster-Than-Nyquist (FTN) signaling is an innovative approach that enables the transmission of data symbols at rates exceeding Nyquist's signaling rate, thereby utilizing available bandwidth more efficiently. This technique introduces intentional Inter Symbol Interference (ISI) by overlapping symbol pulses, resulting in a non-orthogonal transmission scheme. By trading bandwidth for processing complexity, FTN signaling enables higher data transmission rates within the same allocated bandwidth.

While mobile telephony has evolved beyond voice communication systems, the exponential growth in bandwidth demand has necessitated exploring new approaches. Solid-state technology advancements and computational capabilities have enabled bandwidth trading for increased computational complexity in modern systems.

Mazo initially proposed the concept of FTN signaling in 1975 [1]. However, owing to the complexity associated with the transceiver at the time, its practical implementation was delayed until recently. This parallels the evolution of Low-Density Parity Check (LDPC) codes [2], which were introduced in 1962 but remained unexplored for nearly three decades because of their inherent complexity. In FTN signaling, bandwidth efficiency is achieved by transmitting data symbols faster than Nyquist's orthogonality criterion while maintaining a fixed Power-Spectral Density (PSD). This intentional introduction of controlled ISI can be effectively mitigated using the computational power of solid-state technologies.

The emergence of FTN as an upcoming option for future wireless communications stems from its ability to transmit significantly more data, ranging from 30% to 100%, within the same bandwidth, power, and error rate compared to conventional Nyquist orthogonal signaling schemes. Owing to the increased symbol speed in FTN signaling, the received symbol sequence exhibits severe memory-L ISI, where L represents the length of the FTN channel. Consequently, simple symbol-by-symbol detectors are insufficient for error-free data recovery. A more effective trellis-based detector, such as turbo equalization, is required to separate the most recent symbol from previously transmitted symbols. Turbo equalization employs iterative equalization and decoding of received sequences. Fig. 1 illustrates a common communication link that includes a system setup for a digital transmitter and a turbo equalization receiver. The fundamental components within the transmitter are standard in most communication systems and serve as vital

Manuscript received August 10, 2023; revised October 10, 2023, accepted October 30, 2023; published February 26, 2024.

elements, enabling the application of turbo equalization in the receiver.

This paper focuses on the turbo equalization of FTN ISI channels. The receiver comprises two concatenated blocks: the inner equalizer and outer 5G New Radio (NR) LDPC rate-matched decoder. The equalizer compensates for the ISI present in the received sequence, whereas the decoder performs standard decoding for the 5G NR LDPC code used as an Error-Control Code (ECC).

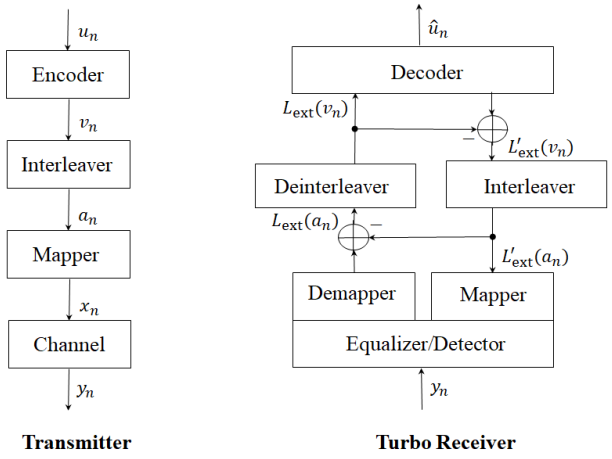

Fig. 1. System configuration and turbo equalization.

Both the equalizer and decoder operate collaboratively by exchanging soft information about the respective symbols, enabling efficient detection processes. Additionally, this study utilizes the 5G NR layered LDPC code as the constituent block for decoding. However, the base graphs specified in the 5G standard have fixed dimensions, enabling only two code rates: 22/68 for base graph 1 and 10/52 for base graph 2. Thus, rate-matching techniques are required to tailor the 5G NR LDPC code to specific desired code rates for transmission. This paper presents various effective and straightforward methods for achieving rate-matching of LDPC codes using bit-puncturing. The rate-matched 5G NR LDPC codes are applied as coding/decoding blocks within the context of turbo equalization for FTN signaling systems. The main contributions of the paper can be summarized as follows:

- We introduce the techniques of message-bit and parity-bit puncturing for the 5G NR LDPC base matrices to generate rate-matched codes in the context of FTN signaling over additive white Gaussian channels.
- The rate-matched LDPC codes are then tested and simulated for different rates.
- Furthermore, benchmarks with equivalent convolutional codes over the same system setup are presented.
- The obtained simulation results represent a benchmark against comparable signaling schemes.

The remainder of this paper is structured as follows: Section II presents the literature review and related work in the context of 5G LDPC coding and FTN signaling. Section III describes the FTN signaling system and elaborates on 5G NR LDPC codes and their decoders. Additionally, it analyzes the receiver iterations of LDPC-coded FTN systems along with the rate-matching process of LDPC codes through puncturing. Simulation results are presented in Section IV, and finally, Section V draws conclusions based on the findings.

II. Related Work

Researchers have investigated various methods to improve the efficiency of wireless communication systems in terms of data rate. For example, in [3], an algebra-assisted method was proposed to construct quasi-cyclic LDPC codes with the properties of supporting multiple expansion factors and rate compatibility for 5G applications. The authors used an algebraic metric that can be applied to construct the exponent matrices for 5G LDPC codes. In addition, in a different study [4], a pipelined layered quasi-cyclic LDPC decoder for 5G NR wireless communications standard was suggested. Therein, a Combined Min-Sum (CMS) decoding algorithm was used and applied to achieve a high-throughput pipelined layered decoder. Furthermore, Sepehr *et al*. [5] discussed NR LDPC structure, design, key features, and rate-matching via several redundancy versions defined non-uniformly. The investigations confirmed the flexibility and robustness of NR LDPC design. Cerci *et al*. [6] highlighted the use of FTN signaling as a solution to overcome rate loss in short-packet communications. They proposed combining a low-complexity FTN signaling detector with nonbinary low-density parity-check codes. Additionally, Brkic *et al*. [7] explored an optimization method for the shaping pulse design in LDPC-coded FTN systems, considering the number of trellises surviving states in the equalization.

As a matter of fact, Quy *et al*. [8] have surveyed the potentials, technologies, and challenges of the 6G communication networks. Driven by the bandwidth efficient utilization, low-latency, and integration with virtual systems, 6G offers unimaginable possibilities. The authors mainly discussed the main characteristics of the 6G and the emerging technologies such as transmission in the terahertz and visible light spectra. Additionally, concepts like blockchains, smart energy harvest, digital twin, metaverse, and cell-free massive MIMO systems were all elaborated upon and analyzed as emerging solutions for the challenges of 6G systems.

Furthermore, Quy *et al*. [9] proposed a novel Adaptive Gateway Selection Mechanism (AGSM) in the MANET-IoT networks based on three metrics. These metrics are distance, queue length, and responsiveness of gateways. The suggested scheme offered load-balancing for the gateways and in-network of MANETs in the 5G networks.

Interestingly, LDPC codes and their variants will likely be a part of the development of 6G, as indicated by a previous study Wang and Zhao [10]. Thus, as 6G aims to seamlessly integrate IoT devices into the network by accommodating a massive number of low-power and low-complexity devices across diverse use cases [11], LDPC codes and other efficient error correction techniques will play a role in the energy and bandwidth efficiency of IoT devices in 6G networks. In another study [12], the authors

investigated the use of Joint Source-Channel Coding (JSCC) in the 6G networks to satisfy the requirements of ultralow-latency and high energy-efficient communications. The proposed scheme is called the double Low-Density parity-Check (D-LDPC) code. D-LDPC codes use two concatenated LDPC codes in the transmitter. The attained results, using the D-LDPC in 6G networks, exhibit superior bit error rate (BER) performance when the base matrices are optimized using a joint design and optimization algorithm.

III. Materials and Methods

A. System Description

In our analysis, we consider the communications system shown in Fig. 2, which shows that the signaling scheme consists of the interleaving of LDPC-coded bits that undergo linear binary modulation and then they are pulse-shaped and transmitted through an FTN channel.

The baseband mathematical model of linearly modulated symbols is given by [13]

$$s_x(t) = \sum_0^\infty x_n h(t - n\tau T), \tau \leq 1 \quad (1)$$

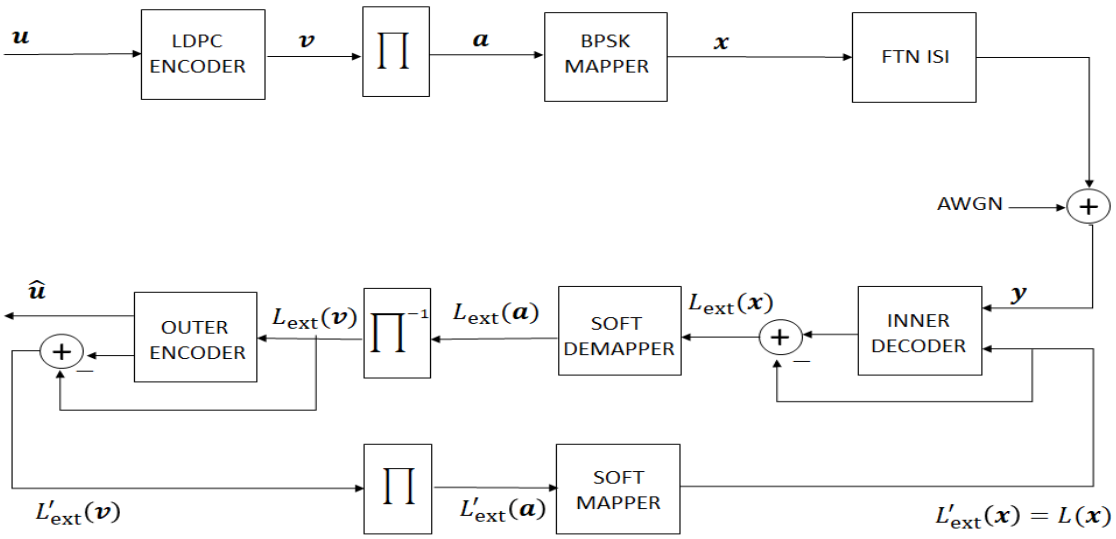

Fig. 2. FTN turbo equalization receiver employing an LDPC decoder.

where x_n denotes real independent and equally likely identically distributed (*i. i. d*) binary data symbols. The pulses, h(t), are T-orthogonal transmission pulses. In Eq. (1), the factor τ represents a packing factor. When $\tau = 1$, the pulses are T-orthogonal, and when $\tau < 1$, the pulses are sped up and form FTN signaling.

In FTN signaling, even when the pulses are sent faster, the minimum Euclidean distance of the signal set remains the same up to a certain limit. Hence, the asymptotic error performance remains unchanged when decoded optimally. Furthermore, while FTN accelerates the transmission pulses, it keeps the PSD of the transmission unchanged.

FTN pulses are transmitted over an Additive White Gaussian Noise (AWGN) channel characterized by a zero mean and a variance of σ^2. The discrete-time representation of the received symbols is

$$\mathrm{y} = \mathrm{x} \times \mathrm{f} + \eta, \quad (2)$$

where η is a random Gaussian sequence with zero mean and an autocorrelation $\phi_\eta(j, j+n) = N_0\delta[n]$, x is the transmitted data symbol, and **f** represents the FTN channel coefficients.

Because the ISI in the received sequence is trellis-structured, in this paper, we apply a receiver that is beyond the simple symbol-by-symbol detector. The receiver applied in this analysis is the suboptimal maximum-likelihood sequence estimation/maximum a posteriori (MLSE/MAP)-based detector for the data acquisition phase.

Although the Iterative (MLSE/MAP) detector is not the optimal approach, it achieves nearly optimal results with tractable complexity. MLSE using the MAP algorithm is used for the turbo equalization of the received FTN signal in Eq. (1). In Fig. 2, L_{ext} denotes the soft information exchanged between the two constituent block decoders in the form of extrinsic log-likelihood ratios (LLRs). The LLRs are further defined later.

In this paper, we adopt the super minimum phase model **f**, presented in previous studies [14, 15], for the 30% root raised cosine (rRC) FTN pulse stretched in time by $\tau = 0.5$. The unit-energy model is

$$f = [-0.005, -0.003, 0.007, -0.011, -0.001, 0.034, -0.019, 0.003, 0.375, 0.741, 0.499, -0.070, -0.214, 0.019, 0.087, -0.020, -0.028, 0.017] \quad (3)$$

The precursor values are expressed in lightface in Eq. (3); all detectors replace these with zeros and operate at a delay K_p. The $\tau = 0.5$ represents a 50% bandwidth reduction of the system. For more material on the FTN, readers can refer to some previous studies [16–19].

Because FTN introduces intentional ISI in the transmitted signal with a memory-L channel response, the receiver design is more complex than the simple symbol-by-symbol detector. As the ISI in the received FTN signal is trellis-structured, an MLSE/MAP-based detector is required. Fig. 2 shows the nearly optimal iterative receiver structure implemented in this analysis for the turbo equalization of the FTN signals in Eq. (2). In the figure, L_{ext} denotes the extrinsic LLRs.

B. Low-Density Parity-Check Codes in the 5G NR Standard

LDPC codes are a class of linear block codes characterized by the notation (n, k), where k represents the number of bits in the data message sequence and n the length of the codeword. LDPC codes are always associated with a parity-check matrix H, which, in the case of LDPC, is sparse, and hence the code is described as low-density. The parity-check matrix is often represented graphically using a bipartite graph called the Tanner graph, as shown in Fig. 3.

$$H = \begin{bmatrix} 1 & 0 & 0 & 1 & 1 & 0 & 1 \\ 0 & 1 & 0 & 1 & 0 & 1 & 1 \\ 0 & 0 & 1 & 0 & 1 & 1 & 1 \end{bmatrix}$$

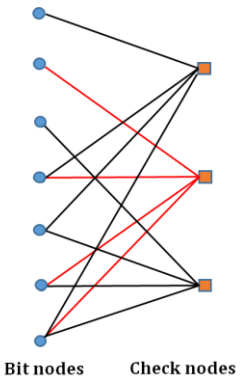

Fig. 3. Graphical representation of a parity-check matrix using a Tanner graph.

The Tanner graph consists of n bit-nodes and $(n-k)$ parity-nodes, where n represents the length of the LDPC codeword C, and k is the length of the message sequence. In the Tanner graph, for the LDPC codewords to be valid, the sum of the code bits connected to each parity node should sum to zero. This can be represented mathematically as follows

$$\boldsymbol{H}.\boldsymbol{C}^{\boldsymbol{T}} = \boldsymbol{0}, \tag{4}$$

where the sparsity of the $\boldsymbol{H}$ -matrix is key to the efficient implementation of the decoding algorithm.

1) LDPC decoding

The process of decoding LDPC codes belongs to a general class of algorithms called message-passing decoders. The reason for this nomenclature is that messages are exchanged between the message and check nodes in the decoder in iterative loops.

An important subclass of the message-passing algorithms is the Belief Propagation (BP) decoding. In BP, messages in the form of beliefs are exchanged iteratively between the message and check nodes, as shown in the Tanner graph in Fig. 3. These beliefs are expressed in terms of extrinsic LLRs, alternatively called soft information, and the entire process is referred to as soft decoding.

The soft decoding process of LDPC codes involves two main steps. The first step is the vertical step, which involves updating the soft information of each of the check nodes. The other step is the horizontal one in which the message nodes update their soft information. The decoding process proceeds by passing the soft information, in the form of extrinsic LLRs, from the check nodes to the bit nodes and vice versa.

For each nonzero entry in the parity-check matrix, let us define $\eta_{m,n}$ as the LLR message sent from check node m to bit node n. The LLR $\eta_{m,n}$ is calculated as follows:

$$\eta_{m,n} = -2\tanh^{-1}\left(\prod_{j\in N_{m,n}}\tanh\left(-\frac{\lambda_j-\eta_{m,j}}{2}\right)\right), \tag{5}$$

where $N_{m,n}$ denotes the positions in the m^{th} row in $\boldsymbol{H}$ except the one in the n^{th} column. In addition, let us define λ_n as the LLR of the bit node n; thus,

$$\lambda(C_n\backslash\vec{r}) = L_c r_n + \sum_{m\in M_n}\eta_{m,n}, \tag{6}$$

where L_c is the channel reliability, and r_n is the n^{th} received symbol from the channel.

The value $\lambda(C_n\backslash\vec{r})$ represents the total belief the decoder assumes about bit node C_n, given the received sequence $\vec{r}$. If we employ an iterative decoder, alternating between Eq. (5)–(6), then we must remove from $\lambda(C_n\backslash\vec{r})$ the message that it has already received from that check node $\eta_{m,n}$. This represents the extrinsic information passed by the decoder. Using the above iterative decoder, when the decoder reaches the last iteration, Eq. (6) is used to make decisions about the code bit, and the loop terminates.

2) LDPC base matrices in the 5G new radio standard

The 5G NR standard for LDPC codes specifies the LDPC parity-check matrix using the base graph and expansion approach. The standard contains two main base graphs and many choices of expansion factors [20]. By combining a base graph with the appropriate choice of expansion, we can obtain a wide variety of sparse parity-check matrices.

The standard has either base graph 1 (BG1), which has a size of 46×68, or base graph 2 (BG2) with a size of 42×52. For either BG1 or BG2, the base graph matrix has the following block structure: $\begin{bmatrix} \boldsymbol{A} & \boldsymbol{E} & \boldsymbol{O} \\ \boldsymbol{B} & \boldsymbol{C} & \boldsymbol{I} \end{bmatrix}$.

For BG1, submatrix A has dimensions 4×22, E has 4×4, O is an all-zero submatrix with dimensions 4×42, B has 42×22, C has 42×4, and I is a 42×42 identity matrix. For BG2, submatrix A has dimensions 4×10, E has 4×4, O is an all-zero submatrix with dimensions 4×38, B has 38×10, C has 38×4, and I is a 38×38 identity matrix. In both BG1 and BG2, submatrix E has a double-diagonal structure; this is very beneficial for the encoding process.

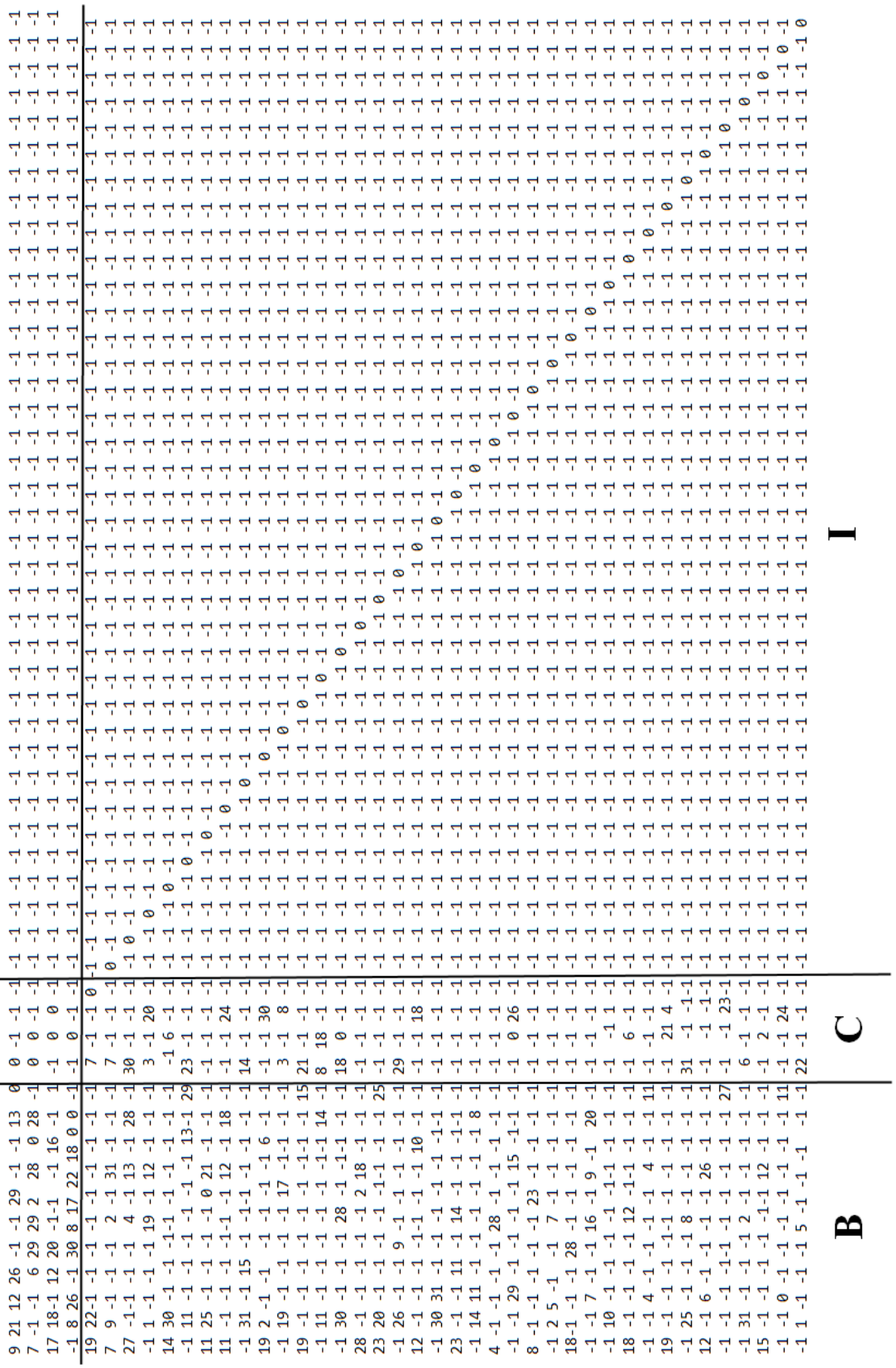

Fig. 4. Base matrix from BG2 and an expansion factor of 32.

The code rates for both BG1 and BG2 are presented below, respectively,

$$R = \frac{k}{n} = \frac{68-46}{68} = \frac{22}{68}, \quad (7)$$

$$R = \frac{k}{n} = \frac{52-42}{52} = \frac{10}{52}, \quad (8)$$

where k represents the number of message bits and n the number of codeword bits. Considering the code rates of BG1 and BG2, we observe that the code rate of BG2 is less than that of BG1; therefore, we expect that running the code using parity-check matrices from BG2 will provide better performance results owing to the more redundancy involved in BG2 [21–24]. An example of a base matrix generated from BG2 and an expansion factor of $z = 32$ is shown in Fig. 4.

In Fig. 4, the expansion factor z is 32; therefore, the entries of the base matrix take values -1, 0, 1, …, 31. These numbers are then replaced by 32×32 matrices as follows:

- The number -1 is replaced by a 32×32 all-zero matrix.
- Any other number i in [0, 31] is replaced by a 32×32 identity matrix shifted right i times.

C. Receiver Iterations of LDPC-Coded Faster-Than-Nyquist Signaling

The serial concatenation setup of an inner equalizer followed by an outer LDPC decoder performs two types

of iterative tasks in the detection process. The first iterative loop is performed between the inner equalizer and the outer decoder. The second loop is performed internally within the LDPC decoder and is referred to as the internal loop.

Considering the outer loop between the equalizer and the decoder, it starts at the inner equalizer, where it calculates its beliefs about each code bit x_n; subsequently, these beliefs are sent from the equalizer to the outer decoder. In addition, the decoder calculates its own beliefs about each code bit and then sends them back to the inner equalizer, and the loop is performed iteratively for a predetermined number of times.

The soft information exchanged between the equalizer and decoder is called the extrinsic LLRs $L_{ext}(\boldsymbol{x})$. The extrinsic LLRs sent from the FTN equalizer are calculated as follows [25]:

$$L_{ext}(x_n) \triangleq \log\left(\frac{P_r(x_n=+1/\vec{r})}{P_r(x_n=x/\vec{r})}\right) - \log\left(\frac{P_r(x_n=+1)}{P_r(x_n=x)}\right), x \in \Omega, \quad (9)$$

where the first term in the above equation represents a posteriori LLRs generated by the equalizer. The second term in (9), which is denoted as $L(x_n)$, represents the a priori LLRs. The a priori LLRs represent prior information on the occurrence probability of x_n, and is provided by the decoder. For the initial equalization step, no a priori information is available and hence we obtain $L(x_n) = 0, \forall n$. The extrinsic LLRs in (9), $L_{ext}\ (x_n)$, are independent of the a priori information, $L(x_n)$, and are sent to the LDPC decoder as a priori information. They are used at the decoder to update the bit nodes, and then the internal LDPC iterative loop starts. It proceeds back and forth between the check and bit nodes for a prescribed number of loops. When the LDPC decoder iterations stop, the extrinsic LLRs in Eq. (6) are sent back to the FTN equalizer as a priori information, etc.

D. Rate-matching and Puncturing in LDPC Codes the subject of rate matching in 5G NR LDPC codes is of particular significance. The available base graphs in the 5G NR standard are BG1 and BG2. The dimensions of BG1 and BG2 are 46×68 and 42×52, respectively. The generation of any LDPC code using the 5G NR parity-check matrix would require using either BG1 or BG2 with an appropriate expansion factor z. Employing a parity-check matrix using BG1 and any value of z would provide a fixed code rate of $\frac{1}{3}$. When using BG2, a fixed rate of $\frac{1}{5}$ would be attained. Therefore, if any other code rate is desired, the standard cannot provide such a result. Thus, the necessity for rate-matched parity-check matrices are fundamental in the context of 5G NR LDPC coding.

Rate-matching in 5G NR LDPC codes is achieved through bit puncturing, which can be message-bit and/or parity-bit puncturing. For the puncturing of message bits, the initial 2×z columns of the parity-check matrix exhibit relatively high density, as shown in Fig. 5. This implies that numerous parity-check equations rely on the reliability of the first 2×z bits of a codeword C. Consequently, these specific bits, denoted as $[c_i]_{1\le i\le 2z}$, are never transmitted. Failure to puncture the first 2×z columns of the parity-check matrix would result in significant error propagation. However, by puncturing the message bits, an additional 2×z parity bits can be transmitted without affecting the code rate ($R = \frac{k}{n}$), where k represents the number of message bits, and n represents the total number of bits. The receiver still employs the corresponding portion of the parity-check matrix for decoding.

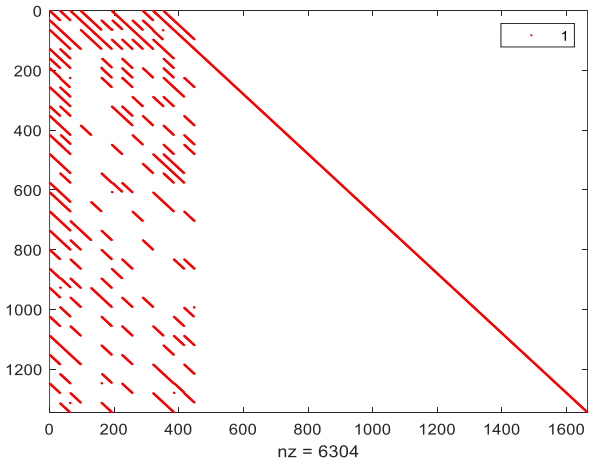

Fig. 5. Distribution of ones in a typical parity-check matrix from the 5G NR standard.

A base graph from BG2 is shown in Fig. 6 where the puncturing of the first columns is indicated in blue. The blue-colored columns are significantly dense compared with the remainder of the base matrix.

Furthermore, puncturing can be applied to the parity bits. By not transmitting the last **P** parity bits of codeword **C**, the effective number of bits, denoted as N, is reduced, which results in an increased code rate R.

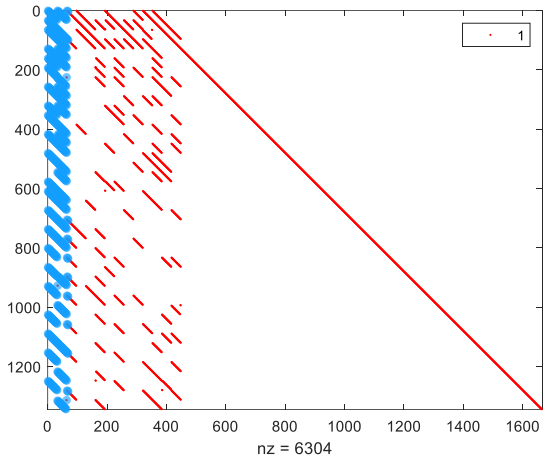

Fig. 6. A depiction of the highly dense first 2z columns (bolded in blue) of a typical parity-check matrix from the 5G NR standard.

For LDPC codes, this technique is referred to as parity-bit puncturing. It can be achieved by disregarding the corresponding rows and columns of the parity-check matrix as displayed by the green-shaded region in Fig. 7.

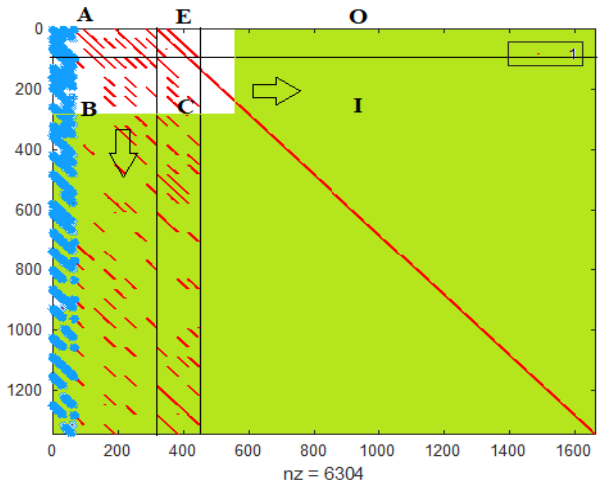

Fig. 7. Graphical description of the parity-bit puncturing of a typical base graph from the 5G NR standard.

The use of only a submatrix of ***H*** reduces the computational cost for encoding and decoding and can therefore increase the throughput for high code rate R. Fig. 7 shows that we can freely extend the green area beyond the **E** submatrix to the right and downwards. By changing the extension that the green area covers, we can tailor the code to the desired k and N, and subsequently, achieve any desired value of code rate.

IV. Result and Discussion

The simulation configuration involved the use of FTN turbo equalization and a binary modulation scheme with a rate-matched LDPC code. The simulations were performed in MATLAB R2019b. The simulation parameters for this work are shown in Table I.

TABLE I. Simulation Parameters

Data packet size	for z=32, block size=704 bits. No.
Modulation scheme	of blocks=100.
Channel type	Binary-PSK
Number of turbo outer iterations	FTN-ISI channel model in (3)
Inner Equalization Parameters	5
MAP detection algorithm	M-BCJR, M=16
LDPC Decoder Parameters	
Base matrices	BG1 and BG2
Applied code rates	$\frac{3}{4}, \frac{1}{2}, and\ \frac{1}{4}$
Number of decoding layers	varies according to the code rate.
Number of decoder internal iterations	1 and 6

The simulations were executed for a total of five outer iterations. The equalizer employed was the M-BCJR algorithm, where the M values were selected to ensure the system complexity was reduced to a small number of states for practical signal-to-noise ratio (SNR) values. The number of internal iterations within the decoder was varied, and the simulation results were recorded at each iteration.

In all the subsequent simulations, a rate-matched LDPC-coded BPSK-modulated signal sequence was transmitted over the AWGN channel at a rate higher than the Nyquist rate by stretching the transmission pulses by $\tau = 0.5$. The simulations were conducted by modifying the code rate at the transmitter and certain parameter values in the serially concatenated turbo equalizer at the receiver.

The received sequence underwent FTN equalization, followed by demodulation and LDPC decoding. Both the equalizer and decoder provided soft information in the form of LLRs. These LLRs were processed through two types of loops: outer loops involving both the equalizer and the decoder, and inner loops specific to the LDPC decoder. In our simulation, we assessed the equalizer's performance by employing varying numbers of iterations for the inner loops.

Furthermore, a diverse set of base matrices was generated from BG1 and BG2 using different expansion factors derived from the 5G standard. The FTN system was tested again using these different base matrices with different rates, and the following simulation results were obtained.

Fig. 8 shows the performance evaluation of FTN equalization for rate-matched LDPC coding, employing a base matrix of BG2, a code rate of $\frac{3}{4}$, and an expansion factor of z=12. The simulation involved five outer turbo iterations and inner iterations of one and six, respectively. The graph presents the performance results in comparison with uncoded binary phase shift keying (BPSK) modulation over an AWGN channel, enabling a comprehensive analysis.

Fig. 8 shows that increasing the number of inner iterations for the LDPC decoder boosted the BER performance significantly compared with the performance attained with one inner iteration only. Additionally, the power of LDPC code is clearly manifested in the figure, where the coded transmission with little redundancy over

an FTN channel could easily outperform its uncoded peer over an AWGN channel.

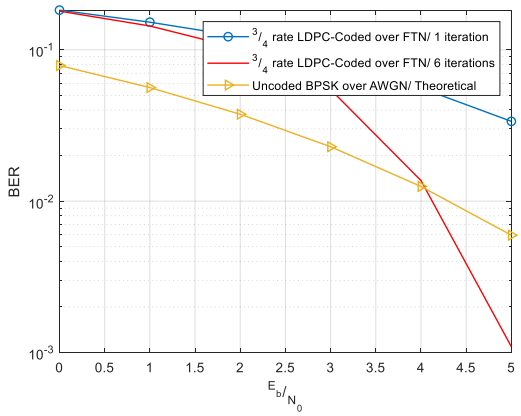

Fig. 8. Performance of a rate $\frac{3}{4}$ 5G NR LDPC code over a $\tau = 0.5$ FTN channel.

As shown in Fig. 9, the amount of redundancy for the rate-matched LDPC code was increased and the code rate became $\frac{1}{2}$. The BER performance improved both for one and six inner iterations compared with those shown in Fig. 8.

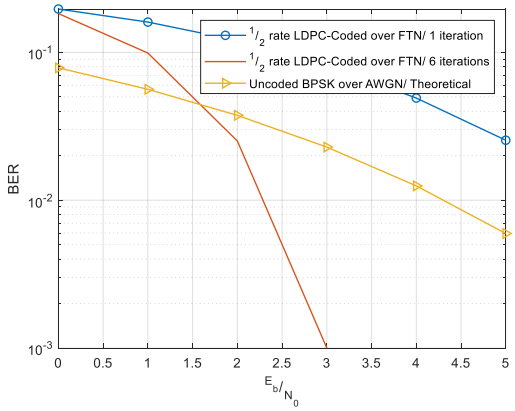

Fig. 9. Performance of a rate $\frac{1}{2}$ 5G NR LDPC code.

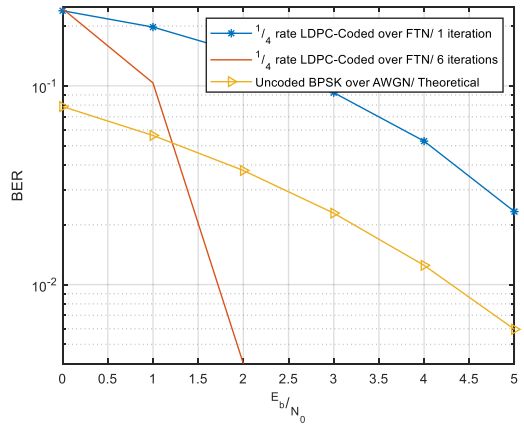

Fig. 10. Performance of a rate $\frac{1}{4}$ 5G NR LDPC code over a $\tau = 0.5$ FTN channel.

It is shown in Fig. 10 that the code rate became smaller and the BER performance became better. Again, we observed increasing the number of LDPC inner iterations is essential to obtaining outstanding performance but with a controlled increase in decoder complexity. In this scheme of LDPC rate matching through both message-bit and parity-bit puncturing, any code rate can be attained from the NR 5G standard to comply with any specific application.

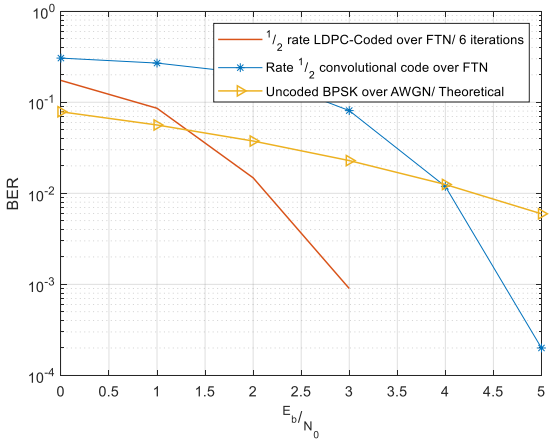

Fig. 11. Comparison between a rate $\frac{1}{2}$ 5G NR LDPC code and a rate $\frac{1}{2}$ convolutional code over a $\tau = 0.5$ FTN channel.

Fig. 11 compares a rate–$\frac{1}{2}$ 5G LDPC code with a rate–$\frac{1}{2}$ convolutional code over the same FTN channel with a stretching factor τ of 0.5. The figure clearly shows that the 5G LDPC code outperformed the convolutional code of the same rate over the same setup of FTN signaling. In both schemes in the figure, the number of outer iterations applied in both systems was five. This advantageous performance of LDPC codes over convolutional codes was at the cost of increased

For a 5G LDPC decoder to perform well, it must run a certain number of inner loops. For FTN signaling with $\tau = 0.5$, a minimum of six inner iterations are required for a satisfactory

performance. In contrast, for convolutional codes, this requirement of inner loops at the decoder does not exist. The existence of layering and inner loops at the LDPC decoder makes LDPC decoders significantly more complex than the convolutional decoder. This complexity increases with the increase in the number of inner iterations. For turbo equalization over FTN signaling with the use of convolutional codes as the outer constituent block, the only loops employed are the outer loops that run between the outer decoder and the BCJR equalizer. While these outer iterations also hold for the FTN equalization employing LDPC codes, additional inner loops within the decoder itself are required, which increases the complexity considerably.

V. Conclusion

This paper has presented a comprehensive study on the use of message-bit and parity-bit puncturing to achieve rate-matching in the context of NR 5G LDPC coding. The

rate-matched coded sequences were successfully transmitted over an FTN channel with a stretching factor τ=0.5, hence, doubling the transmission speed. The simulations conducted showed that we can rate-match the 5G NR LDPC code to any specific application while retaining a desired level of bit-error performance. The attained results are compared with a similar rate convolutional code over FTN transmission, and the former outperforms the latter in terms of BER performance. The trade-off to this outperformance of the LDPC codes has a cost of additional complexity imposed by the iterative layered LDPC decoder at the receiver. However, the benefits gained in terms of improved error control make this trade-off worthwhile. The flexibility of generating codes with different rates from the base matrices, coupled with the superior BER performance, positions LDPC codes as a highly promising solution for efficient and reliable communication in FTN systems and makes the 5G NR LDPC codes further researched in the future.

Conflict of Interest

The authors declare no conflict of interest.

Author Contributions

Asma A. Alqudah: Conceptualization, methodology, formal analysis, software, writing-original draft, writing-review & editing, visualization, and supervision; Khaled F. Hayajneh: Investigation, resources, data curation, writing-review & editing, visualization, and supervision; Hazim M. Shakhatreh: Investigation, resources, data curation, writing-review & editing, visualization, and supervision; Hasan A. Aldiabat: Investigation, resources, data curation, writing-review & editing, visualization, and supervision; all authors had approved the final version.

References

[1] J. E. Mazo, "Faster-than-Nyquist signaling," *Bell System Technical Journal*, vol. 54, no. 8, pp. 1451–1462, Oct. 1975.

[2] R. Gallager, "Low-density parity-check codes," *IRE Transactions on Information Theory*, no. 1, pp. 21–28, 1962.

[3] H. Li, B. Bai, X. Mu, J. Zhang, and H. Xu, "Algebra-assisted construction of quasi-cyclic LDPC codes for 5G new radio," *IEEE Access*, vol. 6, pp. 50229–50244, 2018.

[4] T. B. Nguyen, T. N. Tan, and H. Lee, "Low-complexity high-throughput QC-LDPC decoder for 5G new radio wireless communication," *Electronics*, 2021, vol. 10, p. 516.

[5] F. H. Sepehr, A. Nimbalker, and G. Ermolaev, "Analysis of 5G LDPC codes rate-matching design," in *Proc. 2018 IEEE 87th Vehicular Technology Conference (VTC Spring)*, Porto, Portugal, 2018, pp. 1–5.

[6] E. Cerci, A. Cicek, E. Cavus, E. Bedeer, and H. Yanikomeroglu, "Coded faster-than-Nyquist signaling for short packet communications," in *Proc. 2021 IEEE 32nd Annual International Symposium on Personal, Indoor and Mobile Radio Communications (PIMRC)*, p. 428 *Proc.* 433, 2021.

[7] S. Brkic, P. Ivanis, and A. Radosevic, "Faster than Nyquist signaling with limited computational resources," *Physical Communication*, vol. 47, 2021, p. 101403.

[8] V. K. Quy, A. Chehri, N. M. Quy, N. D. Han, and N. T. Ban, "Innovative trends in the 6G Era: A comprehensive survey of architecture, applications, technologies, and challenges," *IEEE Access*, vol. 11, pp. 39824–39844, 2023.

[9] V. K. Quy, N. T. Ban, D. Van Anh, N. M. Quy and D. C. Nguyen, "An adaptive gateway selection mechanism for MANET-IoT applications in 5G networks," *IEEE Sensors Journal*, vol. 23, no. 19, pp. 23704–23712, 2023.

[10] S. Wang and C. Zhao, "Advances in error correction techniques for next-generation communication systems," published in IEEE Communications Surveys and Tutorials, 2020.

[11] A. N. Barreto and P. O. Esquivel, "IoT Connectivity in 6G: Achievements and challenges," in *Proc. 2020 IEEE Wireless Communications and Networking Conference (WCNC)*, 2020.

[12] Y. Dong, J. Dai, K. Niu, S. Wang, and Y. Yuan, "Joint source-channel coding for 6G communications," *China Communications*, vol. 19, no. 3, pp. 101–115, March 2022.

[13] L. Joiner and A. Alqudah, "Nonbinary coded higher-order modulation in faster-than-Nyquist signaling," *International Journal of Computer Applications and Information Technology*, vol. 9, July 2016.

[14] J. B. Anderson and A. Prlja, "Turbo equalization and an M-BCJR algorithm for strongly narrowband intersymbol interference," in *Proc. 2010 International Symposium on Information Theory and Its Applications*, pp. 261–266, 2010.

[15] A. D. Liveris and C. N. Georghiades, "Exploiting faster-than-Nyquist signaling," *IEEE Transactions on Communications*, vol. 51, no. 9, pp. 1502–1511, 2003.

[16] J. B. Anderson, F. Rusek, and V. Öwall, "Faster-than-Nyquist signaling," in *Proc. IEEE*, vol. 101, no. 8, pp. 1817–1830, Aug. 2013.

[17] M. Ganji, X. Zou, and H. Jafarkhani, "On the capacity of faster than nyquist signaling," *IEEE Communications Letters*, vol. 24, no. 6, 2020.

[18] Y. G. Yoo, and J. H. Cho, "Asymptotic optimality of binary faster-than-Nyquist signaling," *IEEE Communications Letters*, no. 9, pp. 788–790, 2010.

[19] A. Nakamura, Y. Kumagai, S. Saito, H. Suganuma, K. Kuriyama, Y. Ono, H. Fukuzono, M. Yoshioka, and F. Maehara, "Effectiveness evaluation of FTN signaling in the presence of nonlinear distortion under multipath fading channels," *IEICE Communications Express*, vol. 11, no. 2, pp. 104–110, 2022.

[20] 3GPP TS 38.212. Technical specification group radio access network; NR; multiplexing and channel coding. [Online]. Available: https://portal.3gpp.org/desktopmodules/

[21] M. Baldi, M. C. De Gaudenzi, and F. Chiaraluce, "Rate-matched LDPC codes for satellite communications," in *Proc. IEEE*, vol. 95, no. 11, pp. 2209–2224, Nov. 2007.

[22] J. Bae, A. Abotabl, H. Lin, K. Song, and J. Lee, "An overview of channel coding for 5G NR cellular communications," *APSIPA Transactions on Signal and Information Processing*, vol. 8, 2019.

[23] T. Richardson and S. Kudekar, "Design of low-density parity check codes for 5G new radio," *in IEEE Communications Magazine*, vol. 56, no. 3, pp. 28–34, March 2018.

[24] S. O. L. Moheimani, A. D. S. Jayalath, and J. S. Evans, "Rate-matching for LDPC codes in broadband wireless systems," in *Proc. 2008 IEEE 19th International Symposium on Personal, Indoor and Mobile Radio Communications*, Cannes, France, 2008, pp. 1–5.

[25] M. Tuchler, R. Koetter, and A. Singer, "Turbo equalization: principles and new results," IEEE Transactions on Communications, vol. 50, no. 5, May 2002.